Inorganic Chemistry

ARTICLE

pubs.acs.org/IC

Catalytic Roles of the Metal Ion in the Substrate-Binding Site of Coenzyme B_{12}-Dependent Diol Dehydratase

Takashi Kamachi,[†] Kazuki Doitomi,[†] Masanori Takahata,[†] Tetsuo Toraya,[‡] and Kazunari Yoshizawa*[,†]

[†]Institute for Materials Chemistry and Engineering and International Research Center for Molecular Systems, Kyushu University, Fukuoka 819-0395, Japan

[‡]Department of Bioscience and Biotechnology, Okayama University, Okayama 700-8530, Japan

Supporting Information

ABSTRACT: Functions of the metal ion in the substrate-binding site of diol dehydratase are studied on the basis of quantum mechanical/molecular mechanical (QM/MM) calculations. The metal ion directly coordinates to substrate and is essential for structural retention and substrate binding. The metal ion has been originally assigned to the K^+ ion; however, QM/MM computations indicate that Ca^{2+} ion is more reasonable as the metal ion because calculated Ca−O distances better fit to the coordination distances in X-ray crystal structures rather than calculated K−O distances. The activation energy for the OH group migration, which is essential in the conversion of diols to corresponding aldehydes, is sensitive to the identity of the metal ion. For example, the spectator OH group of substrate is fully deprotonated by Glu170 in the transition state for the OH group migration in the Ca-contained QM/MM model, and therefore the barrier height is significantly decreased in the model having Ca^{2+} ion. On the other hand, the deprotonation of the spectator OH group cannot effectively be triggered by the K^+ ion. Moreover, in the hydrogen recombination, the most energy-demanding step is more favorable in the Ca-contained model. The proposal that the Ca^{2+} ion should be involved in the substrate-binding site is consistent with an observed large deuterium kinetic isotope effect of 10, which indicates that C−H bond activation is involved in the rate-determining step. Asp335 is found to have a strong anticatalytic effect on the OH group migration despite its important role in substrate binding. The synergistic interplay of the O−C bond cleavage by Ca^{2+} ion and the deprotonation of the spectator OH group by Glu170 is required to overcome the anticatalytic effect of Asp335.

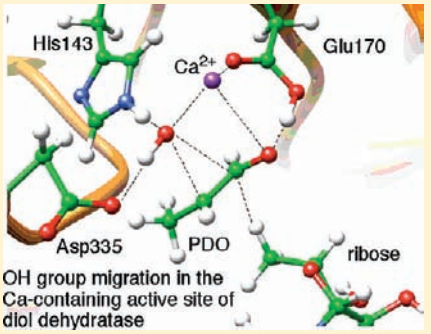

OH group migration in the Ca-containing active site of diol dehydratase

1. INTRODUCTION

Coenzyme B_{12}-dependent diol dehydratase[1,2] catalyzes the conversion of 1,2-diols to corresponding aldehydes. Figure 1 shows a minimal mechanism for this enzymatic dehydration, which involves the hydrogen atom abstraction from C1 and the migration of an OH group from C2 to C1 of 1,2-propanediol (PDO).[3] Adenosyl radical that is generated by the homolytic cleavage of the Co−C covalent bond in adenosylcobalamin (AdoCbl) plays an essential role in this OH group migration. At first, the adenosyl radical abstracts a hydrogen atom from C1 to form 1,2-diol radical (substrate-derived radical), and then the OH group on C2 migrates to C1 leading to the formation of 1,1-diol radical (product-related radical). The resultant 1,1-diol radical abstracts a hydrogen atom from 5′-deoxyadenosine, which leads to the formation of the 1,1-diol and the regeneration of adenosyl radical.

Crystallographic studies[4] of diol dehydratase complexed with adeninylpentylcobalamin have provided important clues to understand the reaction at the molecular level. There is K^+ ion in the inner part of the active site. This K^+ ion is coordinated by five oxygen atoms originated from the side chains of Gln141, Glu170, Glu221, Gln296, and the carbonyl group of Ser362, as shown in Figure 2.

The sixth and seventh coordination positions are occupied by the two hydroxyl groups of the substrate, PDO. The O2 atom of PDO is bonded to COO^- of Asp335 and the Nε2 atom of His143 by a hydrogen bond, and the O1 atom is also bonded to COO^- of Glu170 and the Nε1 atom of Gln296. To reveal the catalytic roles of the K^+ ion in the diol dehydratase reaction, we performed density-functional-theory (DFT) calculations with a simple model involving K^+ ion, propanediol, and ethyl radical.[5] Substrate and the radical intermediates are always bound to K^+ ion in the course of the reaction. However, the lowering of the activation energy by the K^+ ion for the OH group migration is only 2.2 kcal/mol. These results suggest that the most important role of the K^+ ion in the reaction is to fix the substrate and the intermediates in the proper position to ensure the hydrogen abstraction and the OH group migration.

Recently, we built a whole-enzyme quantum mechanical/molecular mechanical (QM/MM) model with 13,500 atoms based on the crystal structure to investigate how the catalytic residues in the substrate-binding site contribute to the hydrogen

Received: November 25, 2010
Published: March 09, 2011

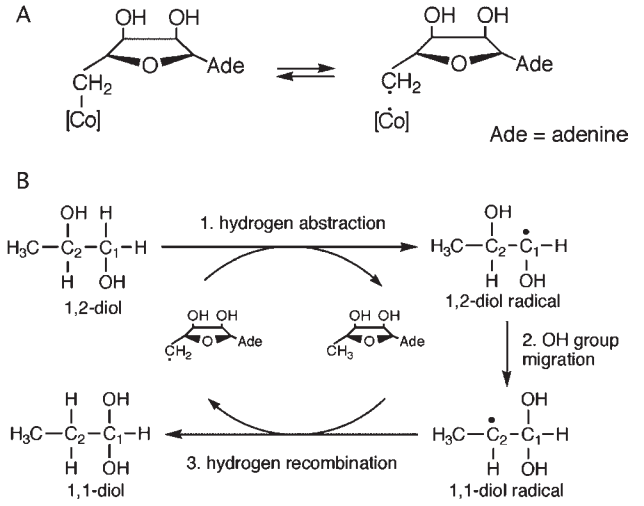

Figure 1. Minimal mechanism of the diol dehydratase reaction. (A) Homolytic cleavage of the Co−C bond in AdoCbl. (B) Adenosyl radical-catalyzed rearrangement.

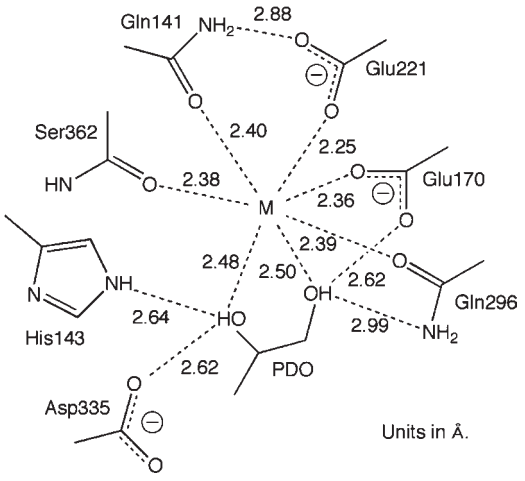

Figure 2. X-ray structure of diol dehydratase.

abstraction and the OH group migration.[6] Surprisingly, the QM/MM-optimized structures have rather long K−O bonds compared with the X-ray structure; K−O1 and K−O2 bonds were calculated to be 2.814 and 2.791 Å, respectively. The error of 0.3 Å is not acceptable in the comparison of X-ray analysis and recent density functional theory. However, we noticed that the calculated K−O distances are typical of potassium-contained complexes. These results led us to re-evaluate the identity of the metal ion in the substrate-binding site from QM/MM computations.[7] We examined K and its neighboring elements in the periodic table, Na, Mg, and Ca, as a candidate for the metal ions. The QM/MM model involving Ca^{2+} ion best matches the X-ray structure with a root-mean-square (rms) error of 0.1 Å. Ca^{2+} ion is the most abundant metal ions found in crystal structures deposited in the Brookhaven Protein Data Bank (PDB). Seven oxygen atom ligands are most frequently arranged in a pentagonal bipyramidal fashion around Ca^{2+} ion at an average Ca−O bond distance of 2.4 Å.[8] These results indicate that the identity of the metal ion in the substrate-binding site of diol dehydratase is most likely to be the Ca^{2+} ion. Very recently, Toraya et al.[9] obtained Ca-deprived diol dehydratase with the ethylenediaminetetraacetic acid (EDTA) treatment, followed by ultrafiltration. The affinity of the Ca-free site for substrate was found to be 500-fold lower than that of Ca-contained active site, which demonstrates that Ca^{2+} ion is directly involved in substrate binding.

Here we investigate catalytic roles of the metal ion in the hydrogen atom abstraction and the OH group migration processes catalyzed by diol dehydratase from QM/MM computations. The QM/MM study demonstrates that the Ca^{2+} ion is more reasonable because the calculated Ca−O distances better fit to the coordination distances in X-ray crystal structures rather than the calculated K−O distances. We find that the Ca^{2+} ion significantly reduces the activation barrier of the OH group migration, because of its strong electron-withdrawing power in contrast to K^+ ion. Thus, the central metal ion in the substrate-binding site does not only serve as an anchor of substrate but also facilitate the OH group migration. In this theoretical work we have the intention to develop a computational mutation analysis for future enzyme chemistry.

2. METHOD OF CALCULATION

We built a QM/MM model of diol dehydratase based on the crystal structure of diol dehydratase-adeninylpentylcobalamin complex with the highest resolution (PDB ID 1EEX). Toraya and co-workers[4] found that it is not possible to superimpose the structure of adenosyl cobalamin on that of adeninylpentylcobalamin in the X-ray crystal structure without the cleavage of the Co−C bond. This result indicates that marked strains must be induced to cleave the Co−C bond, the bond dissociation energy (BDE) of which is experimentally[10,11] and theoretically[12−17] estimated to be about 30 kcal/mol. The C1 atom of the substrate is 6.6 Å apart from the radical center C5′ in the model structure. Although this distance is too far for the radical transfer from the substrate to the adenosyl radical, the C5′-centered radical of the adenosyl group becomes accessible to the *pro-S* hydrogen atom to be cleaved on the C1 of the substrate by rotating the ribose moiety around the glycosidic linkage.[4] On the basis of these findings, we manually replaced the pentyl moiety of the X-ray crystal structure with ribose.

2-1. System Setup. Protonation states of titratable residues at pH 8 were determined with the Generalized-Born method.[18−20] The protonation states were cross-checked with another pK_a prediction program, PROPKA.[21] To reduce the computational cost for QM/MM calculations, the size of the entire system has to be reduced: the constructed enzyme model includes ligands, water molecules, and all amino acids that have atoms within a distance of 30 Å around any atom of substrate, resulting in 12754 atoms in total. The dangling bonds at the boundary are capped with hydrogen atoms. The system was heated and equilibrated at the CHARMm[22,23] level of theory in three steps: (i) steepest descent optimization of the system to eliminate bad contacts (rms gradient <0.1 kcal/mol^{-1} Å^{-1}), (ii) molecular dynamics (MD) for 15 ps heating from 50 to 300 K with the leapfrog Verlet integrator, and (iii) equilibration for 400 ps at 300 K with a time step of 1 fs. During the initial optimization and the classical MD simulation the coordinates of the QM-region atoms defined in the section 2-2 and of heavy atoms beyond 20 Å from any atom of substrate were kept fixed at the X-ray coordinates to preserve the X-ray structure. The coordinates of the corrin ring were also fixed at the X-ray crystal structure. We used CHARMm parameters for cobalamin reported in our previous work. The SHAKE algorithm[24] was used to constrain bonds involving hydrogen atoms. Finally, we extracted the final structure (400 ps) in the equilibration trajectory, which was then minimized with the adopted basis Newton−Raphson (ABNR) algorithm[25] for 5000 steps. All calculations were carried out with Discovery Studio 2.0.[26]

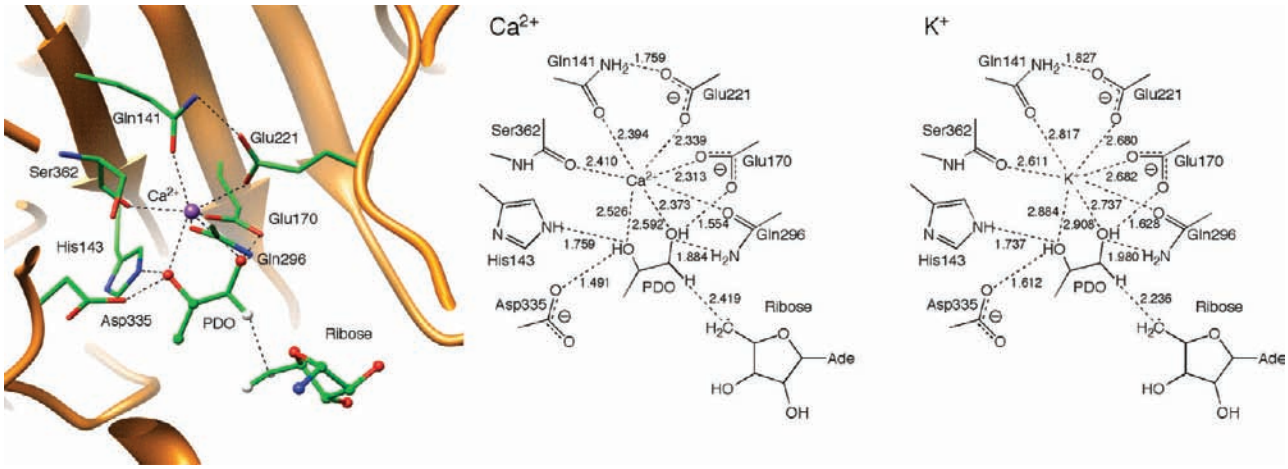

Figure 3. QM/MM optimized structures of the substrate-binding site including Ca^{2+} and K^{+} ion. Units in Å.

2-2. QM/MM Calculations. QM/MM calculations started from the MM-optimized structures obtained in the setup phase. We chose the metal ion, the ribose moiety of adenosyl radical, the side chain of Gln141, His143, Glu170, Glu221, Gln296, Asp335, the carbonyl group of Ser362 and (*S*)-1,2-propandiol (PDO) as the QM region (81 atoms in total). The QM/MM interfaces were placed between Cα and Cβ for the histidine and aspartic acid residues, between Cβ and Cγ for glutamine and glutamic acid residues, between Cα and Cβ, and Cα and N for serine (HN-CO−CH), and between the ribose and adenine ring for adenosyl radical. Link atoms were introduced to saturate the valence of the QM boundary atoms with the L2 scheme,[27] where the link atom does not interact with the MM atoms of the adjacent neutral charge group. All QM/MM calculations were performed with the ChemShell package[28] by using TURBOMOLE[29] for the QM calculations at the B3LYP level of theory, which consists of the Slater exchange, the Hartree−Fock exchange, the exchange functional of Becke,[30] the correlation functional of Lee, Yang, and Parr (LYP),[31] and the correlation functional of Vosko, Wilk, and Nusair.[32] We used the SV(P)[33] basis set on all atoms to carry out geometry optimization. Single-point energies of the optimized structures were computed with the TZVP[34] basis set. A standard electronic embedding scheme[35] was chosen; the fixed MM atomic charges were included into the one-electron Hamiltonian of the QM calculations, and the QM/MM electrostatic interactions were evaluated from the QM electrostatic potential and the MM atomic charges. The complete nonbonding MM and QM/MM interactions were calculated without employing any cutoff. The CHARMm force field[22,23] run through the DL_POLY program[36] was used for the MM part of the system. We defined a region with 824 atoms to be fully optimized by including all residues that have atoms within a distance of 10 Å around any atom of substrate, while we kept the remaining atoms fixed. A larger optimized region with 2810 atoms within the 15 Å sphere is also investigated to assess the influence of the outer MM region. As summarized in the Supporting Information, the minimization of the extended MM region essentially has no impact on the relative energies of reaction intermediates. The coordinates of the corrin ring were also fixed at the X-ray structure. It is unlikely that the calculated energies are significantly affected by the fixations. The distance between the metal ion and the Co atom of corrin ring is 12 Å in the X-ray structure, and therefore, cobalamin acts solely as a spectator in the hydrogen transfer and OH group migration.[37] A microiterative scheme was employed to locate transition states of the large system: the system was divided into a reaction core and its environment. A Hessian eigenmode-following algorithm (P-RFO) was used to optimize the reaction core, while the environment was optimized with the L-BFGS algorithm.[38] The nature of the transition states as first-order saddle points was confirmed by numerical frequency calculations. There are many local minima in the large QM/MM model, and therefore, it is important to make sure that the MM regions of the all stationary points are minimized to the same local minima. As summarized in the Supporting Information, we carried out a series of optimizations from a transition state iterating back and forth between all stationary points until the convergence of QM/MM energies (<1 kcal/mol). The QM/MM and QM energies are also summarized in the Supporting Information.

Table 1. QM/MM Optimized Metal−Oxygen Bond Lengths (Å) in the Substrate-Binding Site at the QM (B3LTP/SV(P))/MM (CHARMm) Level of Theory

	Ca^{2+}	K^{+}	X-ray
O1 (PDO)	2.592	2.908	2.50
O2 (PDO)	2.526	2.884	2.48
Gln141	2.394	2.817	2.40
Glu170	2.313	2.682	2.36
Glu221	2.339	2.680	2.25
Gln296	2.373	2.737	2.39
Ser362	2.410	2.611	2.38
rms[a]	0.06	0.37	

[a] RMS errors from experimental values (PDB ID 1EEX).

3. RESULTS

Figure 3 shows QM/MM optimized structures of the substrate-binding site including Ca^{2+} and K^{+} ions. There is a sharp contrast between calculated metal−oxygen bond lengths of the two structures.

Table 1 shows QM/MM optimized metal−oxygen bond lengths in the substrate-binding site at the QM (B3LYP/SV(P))/MM (CHARMm) level of theory. Calculated Ca−O bond lengths for the QM/MM model having Ca^{2+} ion inside are in excellent agreement with those of the X-ray structure with a root-mean-square (rms) error of 0.06 Å, whereas K−O bond lengths for the QM/MM model having K^{+} ion inside are much longer than those of the X-ray structure with a rms error of 0.37 Å. This result is in good agreement with our previous conclusion[7] that the identity of the metal ion in the substrate-binding site is most likely to be Ca^{2+}

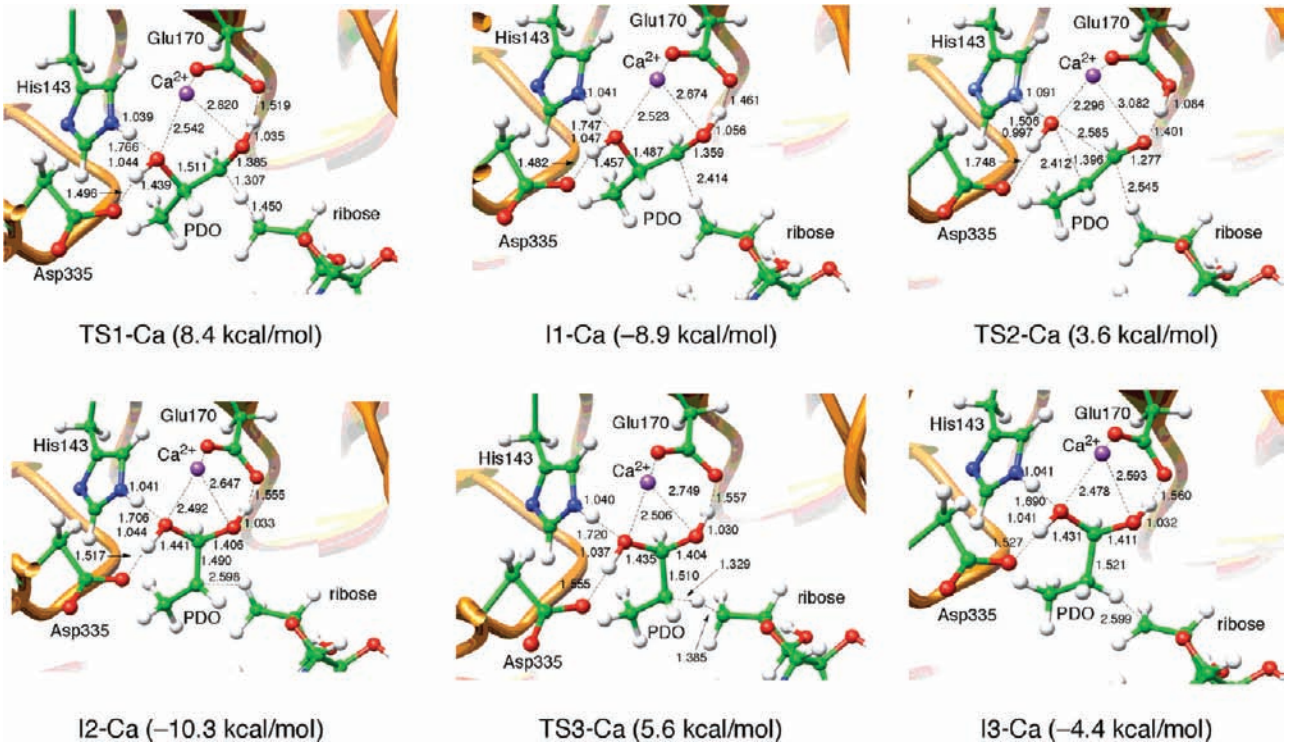

Figure 4. Optimized geometries of intermediates and transition states for the hydrogen abstraction, the OH group migration, and the hydrogen recombination in the Ca-containing model. Units in Å. Relative energies are measured from the initial complex shown in Figure 3.

ion rather than K^+ ion. As indicated earlier in this paper, this prediction was experimentally confirmed by Toraya et al.[9]

3-1. Hydrogen Abstraction. As shown in Figure 3, adenosyl radical generated from the Co−C bond cleavage comes into contact with the *pro-S* hydrogen atom to be abstracted in the initial stages of the reaction. The adenosyl radical is rather close to the hydrogen atom in the K-contained model; the distance between the *pro-S* hydrogen atom and the C5′ atom is calculated to be 2.419 and 2.236 Å in the QM/MM models including the Ca^{2+} and K^+ ions, respectively. This difference is a direct consequence of the longer K−O1 and K−O2 bond lengths. The activation barrier for the hydrogen abstraction is of course sensitive to the distance, as proposed in our computational mutation study[39] of diol dehydratase. Figures 4 and 5 show QM/MM optimized geometries of the intermediates and transition states for the hydrogen abstraction, the OH group migration, and the hydrogen recombination steps in the QM/MM model including the Ca^{2+} and K^+ ions, respectively. We present only the metal ion, the substrate, the ribose moiety, His143, Glu170, and Asp335 for clarity in the figures. The activation barrier of 8.4 kcal/mol for the hydrogen atom transfer in the Ca-contained model (**TS1-Ca**) is 3.1 kcal/mol higher than the corresponding barrier in the K-contained model (**TS1-K**), as expected from the short distance between the *pro-S* hydrogen atom and the C5′ atom in the initial complex. This barrier reduction is mainly ascribed to the MM energy difference of the protein, as shown in Table 2. We evaluated the MM contribution of amino acids in the MM region to find important residues in reducing the activation barrier for the K-contained model (Supporting Information, Table S1 and Figure S2). The major MM energy term comes from Glu168, Gln200, Lys255, Ser333, and Ser361. These residues are located close to the QM region, especially to Gln141, Glu170, and Asp335. The distances between these residues and the QM atoms in the K-contained model are shortened in comparison with those in the Ca-contained model because of the longer K−O bond lengths. Thus, the MM contributions in the K-contained model are sensitive to the geometrical changes of the QM region in the course of reaction (2.7 kcal/mol barrier reduction), whereas the MM energies in the Ca-contained model do not significantly affect the barrier (only 0.7 kcal/mol). **TS1-Ca** (**TS1-K**) has a C1−H bond of 1.307 (1.271) Å and a C5′−H bond of 1.450 (1.503) Å; these bond distances as well as a linear arrangement of the C−H−C moiety are a typical feature in the C−H bond activation in various reactions.[40] In the resultant 1,2-diol radical (**I1-Ca** and **I1-K**), the hydrogen bond between the spectator OH group and Glu170 are remarkably changed compared with the initial complex; the O1−H bond distance increases by 0.029 (0.025) Å and the O (Glu170)−H bond distance decreases by 0.093 (0.104) Å in **I1-Ca** (**I1-K**). This intermediate is an α-hydroxyl radical species, which is up to 10^5 times more acidic than corresponding alcohols.[41−43] The anionic carboxyl group of Glu170 attracts the partially activated hydroxyl proton of the 1,2-diol radical, which would reduce the activation barrier for the OH group migration, as discussed later in this manuscript. The bond distance of C1−O1 decreases from 1.417 (1.407) Å in the initial complex to 1.359 (1.354) Å in **I1-Ca** (**I1-K**). This geometrical change is due to the resonance structure possessing O-centered radical and the concomitant C1−O1 double bond. The relative energy of **I1-Ca** (**I1-K**) is −8.9 (−11.6) kcal/mol measured from the initial complex, which shows that the Ca^{2+} ion destabilizes the intermediate by 2.7 kcal/mol compared with the K^+ ion. As discussed in our previous study,[39] the hydrogen-bonding interaction between the spectator OH group and

dx.doi.org/10.1021/ic102352b |*Inorg. Chem.* 2011, 50, 2944–2952

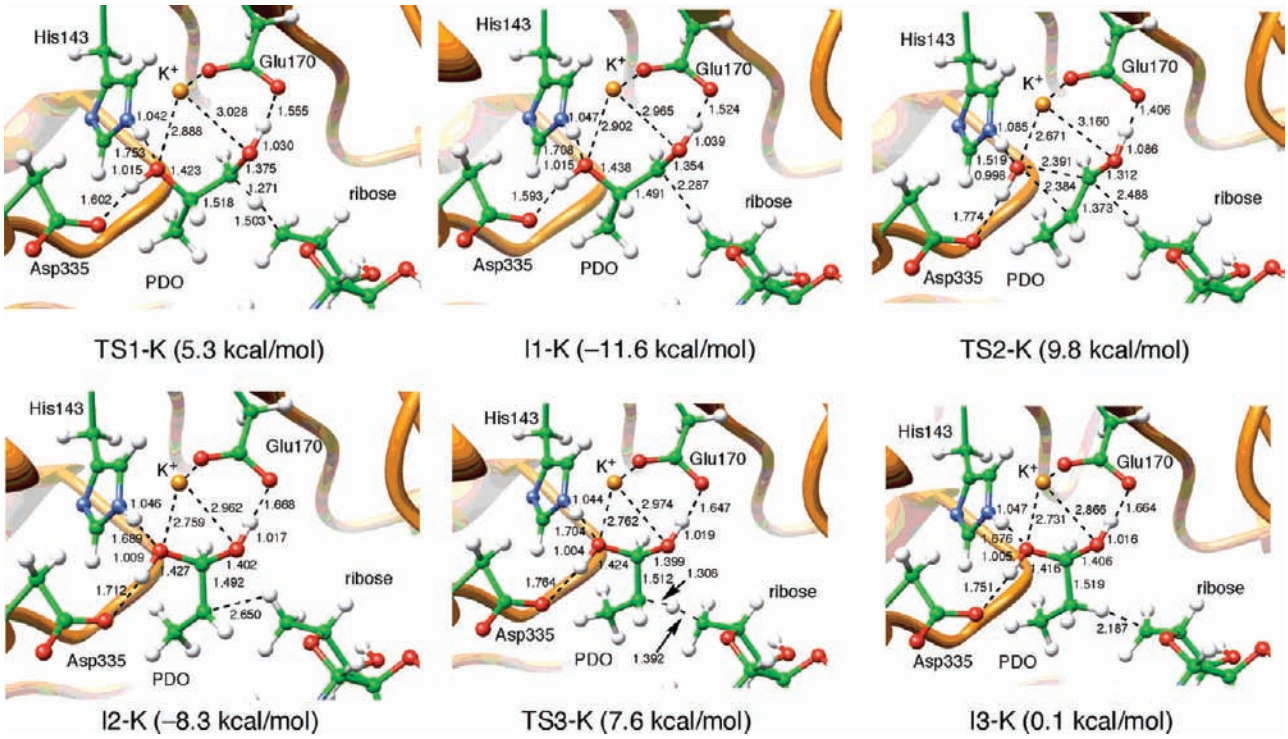

Figure 5. Optimized geometries of intermediates and transition states for the hydrogen abstraction, the OH group migration, and the hydrogen recombination in the K-containing model. Units in Å. Relative energies are measured from the initial complex shown in Figure 3.

Table 2. QM/MM and QM Energies (kcal/mol) Measured from RC

	RC	TS1	I1	TS2	I2	TS3	I3
				K			
QM/MM	0.0	5.3	−11.6	9.8	−8.3	7.6	0.1
QM[a]	0.0	8.0	−11.8	9.2	−5.8	12.3	1.0
				Ca			
QM/MM	0.0	8.4	−8.9	3.6	−10.3	5.6	−4.4
QM[a]	0.0	7.7	−8.6	4.2	−8.2	6.5	−3.5

[a] QM energies with MM point charges.

Glu170 reduces the BDE of the C1−H bond. Thus, the destabilization of **I1-Ca** comes from the strong electron-withdrawing power of the Ca^{2+} ion that weakens the hydrogen-bonding interaction.

3-2. Catalytic Effects of Ca^{2+} Ion in the OH Group Migration. Smith, Golding, and Radom[44] proposed that the barrier height of the OH group migration step is lowered through the partial protonation of the migrating OH group and the partial deprotonation of the spectator OH group. We reported using a simple model involving K^+ ion, propanediol, and ethyl radical that the OH group migration proceeds in a concerted manner with an activation energy of 18.7 kcal/mol and that it is lowered only by 2.2 kcal/mol in the presence of K^+ ion.[5] Here we considered a concerted OH group migration in this QM/MM model having Ca^{2+} and K^+ ion in the substrate-binding site. Several mutants of diol dehydratase were prepared by site-directed mutagenesis for the investigation of the contributions of the amino acid residues in the active site to the catalysis.[45] The Glu221Ala mutant enzyme does not form an $(\alpha\beta\gamma)_2$ complex, which suggests that this mutation indirectly disrupts subunit contacts. The Glu170Ala, Asp335Ala, and Asp335Asn mutants are totally inactive (<0.01%), and the His143Ala mutant shows only 5.1% of activity of the wild-type enzyme, which indicates that Glu170, Asp335, and His143 are catalytic residues. On the basis of the pK_a value determined by PROPKA, we assumed that all titratable residues in the substrate-binding site are deprotonated under the reaction conditions of pH 8.0; the pK_a values of His143, Glu170, Glu221, and Asp335 are −4.71, 7.07, −1.02, and 4.02, respectively. This assumption would be reasonable as judged from the X-ray structure of the enzyme because these residues are located in rather polar environment.

The OH migration proceeds in a concerted manner via a transition state (**TS2-Ca** and **TS2-K**) with a triangular structure in the Ca- and K-contained QM/MM models. In this process of **TS2-Ca**, the COO^- group of Glu170 temporarily accepts a proton from the spectator OH group to effectively form the aldehyde radical species; the O1−H and O (Glu170)−H bond distances are 1.401 and 1.084 Å, respectively. The cleavage of the C−O bond and the deprotonation of the spectator OH group occur simultaneously in **TS2-Ca**. The QM/MM calculations did not yield the deprotonated radical intermediate without the C−O bond cleavage, which would deny the possibility of a stepwise mechanism for the OH group migration. On the other hand, the COO^- group of Glu170 partially, but not completely, activates the O1−H bond of **TS2-K**; the O1−H and O (Glu170)−H bond distances are 1.086 and 1.406 Å, respectively. We found that an energy of 2.9 kcal/mol is required to deprotonate the spectator OH group in contrast to **TS2-Ca**.[46] These results indicate that the barrier of the OH group migration is more effectively reduced by the deprotonation of the spectator OH group for **TS2-Ca** than for **TS2-K**. In addition, the partial protonation of the migrating OH group by His143 is likely to

dx.doi.org/10.1021/ic102352b |*Inorg. Chem.* 2011, 50, 2944–2952

reduce the barrier of the OH group migration. The hydrogen bond between the ε-nitrogen atom of His143 and the migrating OH group is shortened to a similar extent in both models in contrast to the deprotonation of the spectator OH group; 0.241 and 0.189 Å in the Ca- and K-contained QM/MM model, respectively. The activation energy of the OH group migration was calculated to be 12.5 and 21.4 kcal/mol for **TS2-Ca** and **TS2-K**, respectively; thus, the barrier being reduced by the Ca^{2+} ion by 8.9 kcal/mol. Why, then, is the barrier reduced in the Ca-contained QM/MM model? Is the barrier reduction of 8.9 kcal/mol for **TS2-Ca** fully ascribed to the deprotonation of the spectator OH group by Glu170? How about the strong electron-withdrawing effect of the Ca^{2+} ion? To address these questions, we performed additional calculations using a small cluster model and a QM/MM model in which the metal ion is deleted.

We consider the OH group migration using a simple model involving propanediol radical and a metal ion (K^+, Na^+, Ca^{2+}, and Mg^{2+}) at the B3LYP/6-311G* level of theory to evaluate the catalytic ability of the metal ion. To assess possible artifacts due to the difference in the total charge of the system, solvent effect calculations were done with the integral equation formalism for the polarized continuum model (IEF-PCM)[47] as implemented in the Gaussian 03 program[48] with a dielectric constant of 6.0, 20.0, 40.0, 60.0, and 80.0. Figure 6 shows optimized structures of the transition state for the OH group migration in the simple model calculation. As listed in Table 3, the calculated activation barrier is well correlated with the charge state of the metal ion. The barrier height of 21.6 kcal/mol in the absence of metal ion is decreased by about 3 and 15 kcal/mol in the presence of the monovalent (K^+ and Na^+) and divalent (Ca^{2+} and Mg^{2+}) cations, respectively, in the gas phase. These values, however, would be overestimated because of the lack of the anionic amino acid residues coordinating to the metal ion in the gas-phase calculations. The lowering of the barrier by Ca^{2+} ion is only a few kcal/mol, and the barrier is not influenced by K^+ ion in the polarized electrostatic environment. Thus, the strong electron-withdrawing power of Ca^{2+} ion alone cannot sufficiently reduce the barrier of the OH group migration. As discussed later in this paper, a synergistic action of Glu170 and Ca^{2+} ion is essential in sufficiently reducing the barrier of the OH group migration.

We also consider effects of Ca^{2+} ion just by removing it from the substrate-binding site of the QM/MM model. As shown in Figure 7, the structure of the active site is greatly disturbed by the electrostatic repulsion between the anionic amino acid residues and by the reorganization of the hydrogen-bonding network in the substrate-binding site. For example, a new hydrogen bond is formed between the ε-nitrogen atom of Gln296 and the migrating OH group. This result demonstrates that the metal ion is used to anchor substrate and amino acid residues that contribute to the catalysis. Although it is difficult to obtain reasonable data from such a biologically unrealistic model, this model would be useful to gain insight into the catalytic behavior of the metal ion in the substrate-binding site. The activation barrier of the OH group migration for this model was calculated to be 17.5 kcal/mol measured from the 1,2-diol radical intermediate. This value is 5.0 kcal/mol higher and 3.9 kcal/mol lower than those for **TS2-Ca** and **TS2-K**, respectively, which is in qualitatively good agreement with the computational results with the simple model. Interestingly, the spectator OH group is not fully deprotonated by the COO^- group of Glu170 in the transition state of this model, as seen in the K-contained QM/MM model; the O1−H and O (Glu170)−H bond distances are 1.078 and 1.411 Å, respectively. This result implies that the presence of a strong

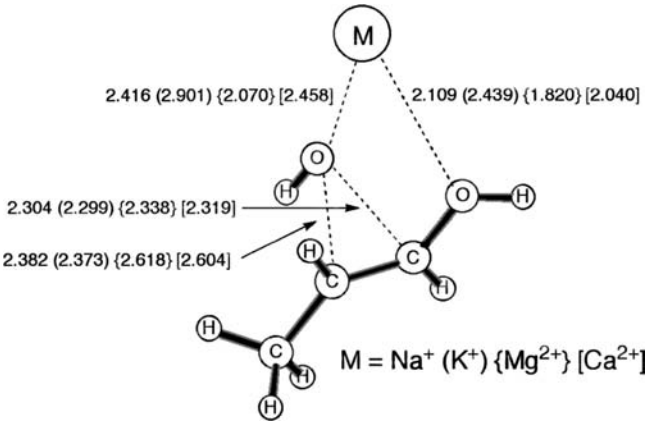

Figure 6. Optimized structure of the transition state for the OH group migration in the simple model calculation. Units in Å.

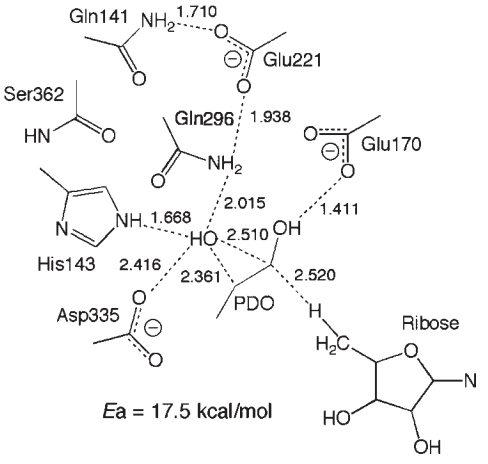

Figure 7. Optimized structure of the transition state for the OH group migration in the QM/MM model without the metal ion. Units in Å.

Table 3. Calculated Activation Barrier (kcal/mol) of the OH Group Migration and Mulliken Charge and Spin Densities on the Migrating OH Group for a Cluster Model Using a Dielectric Constant of 6.0, 20.0, 40.0, 60.0, and 80.0

	ε = 1 (gas)	ε = 6	ε = 20	ε = 40	ε = 60	ε = 80	charge density	spin density
no metal	21.6	22.1	22.3	22.5	22.3	22.3	−0.19	0.69
Na^+	18.8	22.8	23.1	23.2	23.2	23.2	−0.27	0.54
K^+	18.8	22.4	22.7	22.8	22.8	22.8	−0.28	0.54
Mg^{2+}	5.4	19.2	20.9	21.3	21.0	21.7	−0.33	0.26
Ca^{2+}	6.8	19.9	21.5	21.9	22.0	22.0	−0.35	0.27

dx.doi.org/10.1021/ic102352b |*Inorg. Chem.* 2011, 50, 2944–2952

electron-withdrawing metal ion is a prerequisite for the efficient deprotonation of the OH group by Glu170.

3-3. Anticatalytic Effects of Asp335 Ion in the OH Group Migration. The activation barrier for **TS2-K** was calculated to be 11.5 kcal/mol in our previous QM/MM studies.[6] Thus, it is surprising that the OH group migration requires a high activation energy of 21.4 kcal/mol in the present QM/MM calculations. This discrepancy turns out to be primarily due to the choice of the QM region. We newly added Asp335 to the QM region in this study because this residue is hydrogen-bonded to the OH group of the substrate. In fact, the activation energy was estimated to be 14.7 kcal/mol from single-point calculations at the optimized structures of **I1-K** and **TS2-K** when Asp335 is treated at the MM level of theory. Likewise, the activation energy for **TS2-Ca** was calculated to be only 5.9 kcal/mol without Asp335 in the QM region. The COO^- group of Asp335 is hydrogen-bonded to the migrating OH group, as shown in Figure 4. These results indicate that the hydrogen-bonding interaction between Asp335 and the migrating OH group significantly raises the activation barrier of the OH group migration. To examine the effect of a hydrogen-bond acceptor at position Asp335 on the OH group migration, we computed the activation barrier using a simple model in which the Glu170 model ($HCOO^-$) and the Asp335 model (base X) are hydrogen-bonded to the spectator and migrating OH groups, respectively. As shown in Figure 8, the barrier height is increased by 17.3 and 22.1 kcal/mol in the presence of X = $HCOO^-$ and OH^-, respectively. Full deprotonation of the migrating OH group significantly increases the barrier in contrast to that of the spectator OH group. These results are consistent with the previous computational results[49,50] that the partial deprotonation of the migrating NH_3^+ group increases the barrier of the 1,2-shift mediated by ethanolamine ammonia-lyase. From these results, we conclude that Asp335 has a strong anticatalytic effect on the OH group migration despite its important role for substrate binding. The strong electron-withdrawing power of Ca^{2+} ion is likely to be required to compensate the anticatalytic effect of Asp335. Unfortunately, the Asp335Ala mutant is totally inactive despite the absence of the anticatalytic effect since this mutation prevents correct folding of proteins.[45]

3-4. Hydrogen Recombination. Radom and co-workers[51,52] and we[5,39] reported that the activation barrier for hydrogen recombination reactions are slightly larger than those for the initial abstraction reactions and proposed that the hydrogen recombination is the rate-limiting step in the enzymatic reaction. As shown in Figures 4 and 5, the C2 atom of the 1,1-diol radical intermediate, **I2-Ca** and **I2-K**, comes close to the CH_3 group of 5′-deoxyadenosine and abstracts a hydrogen atom from it to lead

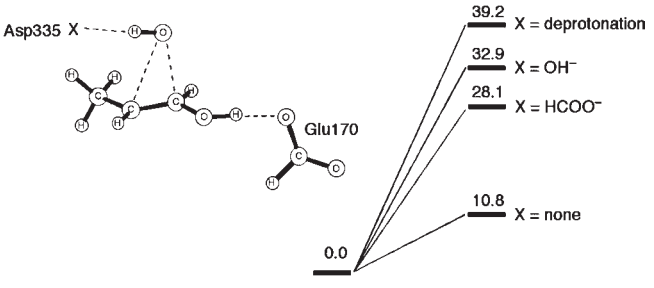

Figure 8. Activation energy (kcal/mol) for the OH group migration catalyzed by the Glu170 model ($HCOO^-$) and the Asp335 model (X) at the B3LYP/6-311G* level of theory.

to the production of the 1,1-diol intermediate, **I3-Ca** and **I3-K**, and to the reproduction of adenosyl radical via **TS3-Ca** and **TS3-K**, respectively. The C2−H and C5′−H bond lengths were calculated to be 1.329 (1.308) and 1.385 (1.392) Å for **TS3-Ca** (**TS3-K**), respectively. The hydrogen recombination is found to be the most energy-demanding step in the Ca-contained model calculations, whereas **TS2-K** is energetically the highest species in the reaction pathway of the K-contained model. The deuterium kinetic isotope effect (KIE) on the overall diol dehydratase reaction is 10, indicating that the breaking of the C−H bond is rate-determining in the reaction.[3a,e,53,54] This result would support our proposal that Ca^{2+} ion is involved in the substrate-binding site of diol dehydratase. The lowering of the activation energy for the OH group migration by K^+ ion is small, while Ca^{2+} ion sufficiently reduces the barrier to explain that the hydrogen recombination is the rate-determining step for the overall reaction. As shown in Table 2, the QM term of TS3 is higher than that of TS2 for both Ca- and K-contained models. This is because the MM part has a different effect on the K-system, decreasing the energy of TS3 by 4.7 kcal/mol, while the energy is only decreased by 0.9 kcal/mol for the Ca-system. The majority of this difference is found to come from Gln200, Ser202, Glu208, Lys255, and Ser333, as shown in the Supporting Information, Table S2 and Figure S3. These residues are likely to reduce the barrier for **TS3-K** in a similar manner as the MM energy term contributes to the reduction of **TS1-K**.

4. DISCUSSION

We have asked at the outset: what is the role of Ca^{2+} ion in the substrate-binding site in the catalysis of diol dehydratase. As concluded in our previous studies,[5] the metal ion acts as an anchor for substrate and catalytic amino acid residues. The structure of the substrate-binding site is significantly disturbed in the absence of the metal ion, as shown in Figure 7. However, this is one aspect of the role of Ca^{2+} ion in the reaction. We found that Ca^{2+} ion directly contributes to the reduction of the barrier height for the OH group migration. The barrier height was calculated to be 12.5 and 21.4 kcal/mol for the transition state in the Ca- and K-contained QM/MM models, respectively; the decrease in the barrier height by 8.9 kcal/mol is significant in catalytic reactions in general. Thus, Ca^{2+} ion is catalytically important for the reduction of the barrier height in the important step. Interestingly, the COO^- group of Glu170 accepts a proton from the spectator OH group in the transition state for the OH group migration in the Ca-contained QM/MM model, whereas the COO^- group of Glu170 partially, but not completely, activates the OH group in the K-contained QM/MM model. Mutational studies[45] of diol dehydratase show that the Asp335Ala mutant is totally inactive, but Asp335 has a strong anticatalytic effect on the OH group migration as opposed to our expectation.

On the basis of these computational results, we present here a comprehensive mechanistic scheme to explain these catalytic roles of the metal ion in the OH group migration. Mulliken charge and spin densities on the migrating OH group in the transition state are −0.47 and 0.30 in the Ca-contained QM/MM model, and are −0.28 and 0.54 in the K-contained QM/MM model, respectively. The OH group has a more radical character in the K-contained model than in the Ca-contained one. This may be viewed as a result from the heterolytic and homolytic cleavage of the O2−C2 bond in the Ca- and K-contained models, respectively. As illustrated in Figure 9, the

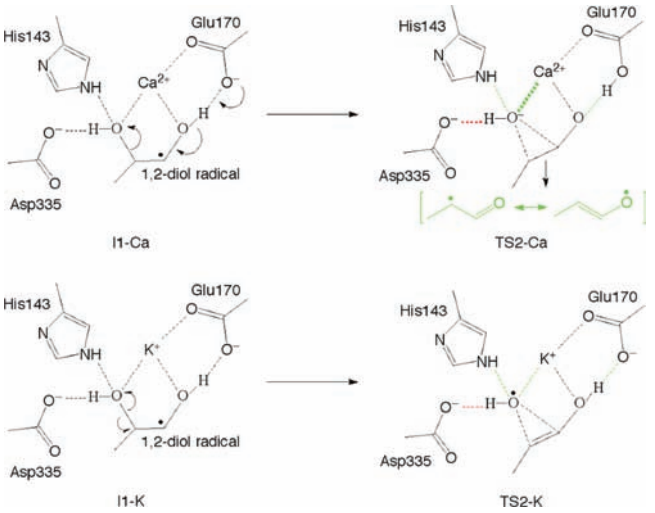

Figure 9. Cartoon showing the electronic changes for the transition state of the OH group migration in the Ca- and K-containing active site of diol dehydratase. Stabilizing and destabilizing effects are colored in green and red, respectively.

O2−C2 bond is heterolytically cleaved by Ca^{2+} ion with its strong electron-withdrawing ability in the transition state. The heterolytic cleavage triggers the full deprotonation of the spectator OH group by Glu170. The high acidity of the spectator OH group is attributed primarily to resonance stabilization of the aldehyde radical moiety of the transition state. As demonstrated in the simple model calculations, only a few kcal/mol lowering of the barrier height by Ca^{2+} ion is observed in the absence of a hydrogen-bond acceptor to the spectator OH group, which shows that Ca^{2+} ion alone cannot sufficiently reduce the barrier of the OH group migration. The synergistic interplay of the heterolytic cleavage of the O−C bond by Ca^{2+} ion and the deprotonation of the spectator OH group by Glu170 is likely to be a key to the barrier reduction for the OH group migration. On the other hand, K^+ ion homolytically cleaves the O2−C2 bond since K^+ ion has a lower electron-withdrawing power, which is not enough to promote the heterolytic cleavage. Consequently, the synergistic action is not operative in the K-contained active site of diol dehydratase, which would significantly increase the activation barrier. The electrostatic repulsion between the migrating OH group and Asp335 leads to an increase in the barrier. The anticatalytic effect of Asp335 is overcome by the strong electron-withdrawing power of Ca^{2+} ion, whereas the OH group migration is interrupted by Asp335 in the K-contained model. The barrier height is 21.4 kcal/mol for the K-contained model. **TS2-K** lies 2.2 kcal/mol above **TS3-K**, which is inconsistent with the observed large deuterium kinetic isotope effects (KIE)[3a,e,53,54] of 10 that indicate the involvement of hydrogen atom transfer in the rate-determining step in the overall reaction. It is proposed that the synergistic action of Glu170 and His143 is necessary for the reduction of the barrier height.[44] However, the barrier height is not sufficiently reduced in the absence of the metal ion even if both Glu170 and His143 work together, as shown in Figure 7. This is because the hydrogen-bonding interaction between the migration OH group and His143 is not strong enough to allow the heterolytic cleavage of the O2−C2 bond; charge and spin densities on the migrating OH group in the transition state are −0.35 and 0.46 in the no-metal QM/MM model. Thus, Glu170 cannot fully deprotonate the spectator OH group in this model. These results imply that the main catalytic partner of Glu170 is not His143 but Ca^{2+} ion in the catalysis of diol dehydratase.

5. CONCLUDING REMARKS

We have studied catalytic roles of the metal ion in the substrate-binding site of diol dehydratase using QM/MM calculations. Ca^{2+} ion is reasonable in the structural aspect and the catalytic function of this enzyme in comparison with K^+ ion that has been experimentally assigned to be located in the metal site. Calculated Ca−O distances better fit the coordination distances in the X-ray structures than the calculated K−O distances. The activation energy for the OH group migration is sensitive to the identity of the metal ion. For example, the spectator OH group of the substrate is fully deprotonated by Glu170 in the transition state for the OH group migration in the Ca-contained QM/MM model; as a result, the barrier height is significantly decreased by the existence of Ca^{2+} ion in the metal site. Moreover, the hydrogen recombination, the most energy-demanding step, is more favorable in the Ca-contained model calculations. Our proposal that Ca^{2+} ion should be involved in the substrate-binding site is consistent with an observed large deuterium kinetic isotope effect of 10, which indicates that C−H bond activation is involved in the rate-determining step. The Asp335 residue is found to have a strong anticatalytic effect on the OH group migration despite its important role in substrate binding. The synergistic interplay of the O−C bond cleavage by Ca^{2+} ion and the deprotonation of the spectator OH group by Glu170 is necessary to overcome the anticatalytic effect of Asp335. These findings based on large-scale quantum chemical calculations encourage us to carry out computational mutation studies in future enzyme chemistry.

■ ASSOCIATED CONTENT

Supporting Information. Energy diagram, two tables and two figures for energy decomposition, two tables for energies, complete ref 48 and XYZ coordinates of the optimized structures. This material is available free of charge via the Internet at http://pubs.acs.org.

■ AUTHOR INFORMATION

Corresponding Author
*E-mail: kazunari@ms.ifoc.kyushu-u.ac.jp.

■ ACKNOWLEDGMENT

K.Y. acknowledges Grants-in-Aid (No. 18GS0207, 18066013, and 22245028) for Scientific Research from JSPS and the Ministry of Culture, Sports, Science and Technology of Japan (MEXT), the Nanotechnology Support Project of MEXT, MEXT Project of Integrated Research on Chemical Synthesis, and CREST of Japan Science and Technology Cooperation for their support of this work.

■ REFERENCES

(1) (a) Dolphin, D., Ed.; In *B12*; John Wiley & Sons: New York, 1982; Vol. 2. (b) Banerjee, R., Ed.; In *Chemistry and Biochemistry of B12*; John Wiley & Sons: New York, 1999.

(2) (a) Toraya, T. *Chem. Rev.* **2003**, *103*, 2095. (b) Toraya, T. *Cell. Mol. Life Sci.* **2000**, *57*, 106.

(3) (a) Zagalak, B.; Frey, P. A.; Karabatsos, G. L.; Abeles, R. H. *J. Biol. Chem.* **1966**, *241*, 3028. (b) Frey, P. A.; Essenberg, M. K.; Abeles, R. H. *J. Biol. Chem.* **1967**, *242*, 5369. (c) Frey, P. A.; Abeles, R. H. *J. Biol. Chem.* **1966**, *241*, 2732. (d) Frey, P. A.; Kerwar, S. S.; Abeles, R. H. *Biochem. Biophys. Res. Commun.* **1967**, *29*, 873. (e) Essenberg, M. K.; Frey, P. A.; Abeles, R. H. *J. Am. Chem. Soc.* **1971**, *93*, 1242. (f) Abeles, R. H.; Lee, H. A., Jr. *Ann. N.Y. Acad. Sci.* **1964**, *112*, 695. (g) Rétey, J.; Umani-Ronchi, A.; Seibl, J.; Arigoni, D. *Experientia* **1966**, *22*, 502. (h) Rétey, J.; Umani-Ronchi, A.; Arigoni, D. *Experientia* **1966**, *22*, 72. (i) Müller, P.; Rétey, J. *J. Chem. Soc., Chem. Commun.* **1983**, 1342. (j) Rétey, J. *Angew. Chem., Int. Ed.* **1990**, *29*, 355. (k) Cockle, S. A.; Hill, H. A. O.; Williams, R. J. P.; Davies, S. P.; Foster, M. A. *J. Am. Chem. Soc.* **1972**, *94*, 275. (l) Finlay, T. H.; Valinsky, J.; Mildvan, A. S.; Abeles, R. H. *J. Biol. Chem.* **1973**, *248*, 1285. (m) Valinsky, J. E.; Abeles, R. H.; Fee, J. A. *J. Am. Chem. Soc.* **1974**, *96*, 4709. (n) Brown, K. L. *Chem. Rev.* **2005**, *105*, 2075.

(4) (a) Shibata, N.; Masuda, J.; Tobimatsu, T.; Toraya, T.; Suto, K.; Morimoto, Y.; Yasuoka, N. *Structure* **1999**, *7*, 997. (b) Masuda, J.; Shibata, N.; Morimoto, Y.; Toraya, T.; Yasuoka, N. *Structure* **2000**, *8*, 775. (c) Shibata, N.; Masuda, J.; Morimoto, Y.; Yasuoka, N.; Toraya, T. *Biochemistry* **2002**, *41*, 12607. (d) Shibata, N.; Nakanishi, Y.; Fukuoka, M.; Yamanishi, M.; Yasuoka, N.; Toraya, T. *J. Biol. Chem.* **2003**, *278*, 22717.

(5) (a) Eda, M.; Kamachi, T.; Yoshizawa, K.; Toraya, T. *Bull. Chem. Soc. Jpn.* **2002**, *75*, 1469. (b) Toraya, T.; Eda, M.; Kamachi, T.; Yoshizawa, K. *J. Biochem. (Tokyo)* **2001**, *130*, 865. (c) Toraya, T.; Yoshizawa, K.; Eda, M.; Yamabe, T. *J. Biochem. (Tokyo)* **1999**, *126*, 650.

(6) Kamachi, T.; Toraya, T.; Yoshizawa, K. *J. Am. Chem. Soc.* **2004**, *126*, 16207.

(7) Kamachi, T.; Takahata, M.; Toraya, T.; Yoshizawa, K. *J. Phys. Chem. B* **2009**, *113*, 8435.

(8) Strynadka, N. C. J.; James, M. N. G. *Curr. Opin. Struct. Biol.* **1991**, *1*, 905.

(9) Toraya, T.; Honda, S.; Mori, K. *Biochemistry* **2010**, *49*, 7210.

(10) Halpern, J.; Kim, S.-H.; Leung, T. W. *J. Am. Chem. Soc.* **1984**, *106*, 8317.

(11) Hay, B. P.; Finke, R. G. *J. Am. Chem. Soc.* **1986**, *108*, 4820.

(12) (a) Hansen, L. M.; Kumar, P. N. V. P.; Marynick, D. S. *Inorg. Chem.* **1994**, *33*, 728. (b) Hansen, L. M.; Derecskei-Kovacs, A.; Marynick, D. S. *J. Mol. Struct. (THEOCHEM)* **1998**, *431*, 53.

(13) (a) Andruniow, T.; Zgierski, M. Z.; Kozlowski, P. M. *J. Phys. Chem. B* **2000**, *104*, 10921. (b) Andruniow, T.; Zgierski, M. Z.; Kozlowski, P. M. *J. Am. Chem. Soc.* **2001**, *123*, 2679. (c) Freindorf, M.; Kozlowski, P. M. *J. Am. Chem. Soc.* **2004**, *126*, 1928. (d) Kozlowski, P. M.; Zgierski, M. Z. *J. Phys. Chem. B* **2004**, *108*, 14163. (e) Kuta, J.; Patchkovskii, S.; Zgierski, M. Z.; Kozlowski, P. M. *J. Comput. Chem.* **2006**, *27*, 1429.

(14) (a) Jensen, K. P.; Ryde, U. *J. Mol. Struct. (THEOCHEM)* **2002**, *585*, 239. (b) Jensen, K. P.; Ryde, U. *J. Phys. Chem. A* **2003**, *107*, 7539. (c) Jensen, K. P.; Ryde, U. *J. Am. Chem. Soc.* **2005**, *127*, 9117.

(15) (a) Dölker, N.; Maseras, F.; Lledós, A. *J. Phys. Chem. B* **2001**, *105*, 7564. (b) Dölker, N.; Maseras, F.; Lledós, A. *J. Phys. Chem. B* **2003**, *107*, 306. (c) Dölker, N.; Maseras, F.; Siegbahn, P. E. M. *Chem. Phys. Lett.* **2004**, *386*, 174. (d) Dölker, N.; Morreale, A.; Maseras, F. *J. Biol. Inorg. Chem.* **2005**, *10*, 509.

(16) Rovira, C.; Kunc, K.; Hutter, J.; Parrinello, M. *Inorg. Chem.* **2001**, *40*, 11.

(17) Kwiecien, R. A.; Khavrutskii, I. V.; Musaev, D. G.; Morokuma, K.; Banerjee, R.; Paneth, P. *J. Am. Chem. Soc.* **2006**, *128*, 1287.

(18) Bashford, D.; Karplus, M. *J. Phys. Chem.* **1991**, *95*, 9556.

(19) Dominy, B. N.; Brooks, C. L., III *J. Phys. Chem. B* **1999**, *103*, 3765.

(20) Spassov, V. Z.; Yan, L. *Protein Sci.* **2008**, *17*, 1955.

(21) (a) Li, H.; Robertson, A. D.; Jensen, J. H. *Proteins* **2005**, *61*, 704. (b) Bas, D. C.; Rogers, D. M.; Jensen, J. H. *Proteins* **2008**, *73*, 765.

(22) (a) Momany, F. A.; Rone, R. *J. Comput. Chem.* **1992**, *13*, 888. (b) Momany, F. A.; Rone, R.; Kunz, H.; Frey, R. F.; Newton, S. Q.; Schäfer, L. *J. Mol. Struct. (THEOCHEM)* **1993**, *286*, 1.

(23) Brooks, B. R.; Bruccoleri, R. E.; Olafson, B. D.; States, D. J.; Swaminathan, S.; Karplus, M. *J. Comput. Chem.* **1983**, *4*, 187.

(24) Ryckaert, J.-P.; Ciccotti, G.; Berendsen, H. J. C. *J. Comput. Phys.* **1977**, *23*, 327.

(25) Press, W. H.; Flannery, B. P.; Teukolshy, S. A.; Vetrrling, W. T. *Numerical Recipes: The Art of Scientific Computing*; University Press: Cambridge, 1987.

(26) *Discovery Studio 2.0*; Accelrys Software Inc.: San Diego, CA, 2007.

(27) Antes, I.; Thiel, W. *Hybrid Quantum Mechanical and Molecular Mechanical Methods*; Gao, J., Ed.; ACS Symposium Series 712; American Chemical Society: Washington, DC, 1998; pp 50−65.

(28) *ChemShell*, a Computational Chemistry Shell; see www.chemshell.org.

(29) Ahlrichs, R.; Bär, M.; Häser, M.; Horn, H.; Kölmel, C. *Chem. Phys. Lett.* **1989**, *162*, 165.

(30) (a) Becke, A. D. *Phys. Rev. A* **1988**, *38*, 3098. (b) Becke, A. D. *J. Chem. Phys.* **1993**, *98*, 5648.

(31) Lee, C.; Yang, W.; Parr, R. G. *Phys. Rev. B* **1988**, *37*, 785.

(32) Vosko, S. H.; Wilk, L.; Nusair, M. *Can. J. Phys.* **1980**, *58*, 1200.

(33) Schäfer, A.; Horn, H.; Ahlrichs, R. *J. Chem. Phys.* **1992**, *97*, 2571.

(34) Schäfer, A.; Huber, C.; Ahlrichs, R. *J. Chem. Phys.* **1994**, *100*, 5829.

(35) Bakowies, D.; Thiel, W. *J. Phys. Chem.* **1996**, *100*, 10580.

(36) Smith, W.; Forester, T. R. *J. Mol. Graphics Modell.* **1996**, *14*, 136.

(37) Buckel, W.; Kratky, C.; Golding, B. T. *Chem.—Eur. J.* **2006**, *12*, 352.

(38) Billeter, S. R.; Turner, A. J.; Thiel, W. *Phys. Chem. Chem. Phys.* **2000**, *2*, 2177.

(39) Kamachi, T.; Toraya, T.; Yoshizawa, K. *Chem.—Eur. J.* **2007**, *13*, 7864.

(40) (a) Yoshizawa, K.; Kamachi, T.; Shiota, Y. *J. Am. Chem. Soc.* **2001**, *123*, 9806. (b) Kamachi, T.; Yoshizawa, K. *J. Am. Chem. Soc.* **2003**, *125*, 4652. (c) Kamachi, T.; Kihara, N.; Shiota, Y.; Yoshizawa, K. *Inorg. Chem.* **2005**, *44*, 4226. (d) Kozlowski, P. M.; Kamachi, T.; Toraya, T.; Yoshizawa, K. *Angew. Chem., Int. Ed.* **2007**, *46*, 980.

(41) Buley, A. L.; Norman, R. O. C.; Pritchett, R. J. *J. Chem. Soc. B* **1966**, 849.

(42) Gilbert, B. C.; Larkin, J. P.; Norman., R. O. C. *J. Chem. Soc., Perkin Trans. II* **1972**, 794.

(43) Hayon, E.; Simic, M. *Acc. Chem. Res.* **1974**, *7*, 114.

(44) (a) Golding, B. T.; Radom, L. *J. Chem. Soc., Chem. Commun.* **1973**, 939. (b) Golding, B. T.; Radom, L. *J. Am. Chem. Soc.* **1976**, *98*, 6331. (c) Smith, D. M.; Golding, B. T.; Radom, L. *J. Am. Chem. Soc.* **1999**, *121*, 5700. (d) Smith, D. M.; Golding, B. T.; Radom, L. *J. Am. Chem. Soc.* **2001**, *123*, 1664. (e) Sandala, G. M.; Smith, D. M.; Radom., L. *Acc. Chem. Res.* **2010**, *43*, 642.

(45) (a) Kawata, M.; Kinoshita, K.; Takahashi, S.; Ogura, K.; Komoto, N.; Yamanishi, M.; Tobimatsu, T.; Toraya, T. *J. Biol. Chem.* **2006**, *281*, 18327. (b) Kinoshita, K.; Kawata, M.; Ogura, K.; Yamasaki, A.; Watanabe, T.; Komoto, N.; Hieda, N.; Yamanishi, M.; Tobimatsu, T.; Toraya, T. *Biochemistry* **2008**, *47*, 3162.

(46) We carried out partial optimization under constraint of the H−O(Glu170) (H−O = 1.085 Å). Only Glu170 and spectator OH group were relaxed in the partial optimization.

(47) (a) Mennucci, B.; Tomasi, J. *J. Chem. Phys.* **1997**, *106*, 5151. (b) Cancès, E.; Mennucci, B.; Tomasi, J. *J. Chem. Phys.* **1997**, *107*, 3032. (c) Cossi, M.; Barone, V.; Mennucci, B.; Tomasi, J. *Chem. Phys. Lett.* **1998**, *286*, 253.

(48) Frisch, M. J. et al. *Gaussian 03*; Gaussian Inc.: Wallingford, CT, 2003.

(49) Wetmore, S. D.; Smith, D. M.; Bennett, J. T.; Radom, L. *J. Am. Chem. Soc.* **2002**, *124*, 14054.

(50) Semialjac, M.; Schwarz, H. *J. Org. Chem.* **2003**, *68*, 6967.

(51) Wetmore, S. D.; Smith, D. M.; Radom, L. *ChemBioChem* **2001**, *2*, 919.

(52) Sandala, G. M.; Smith, D. M.; Coote, M. L.; Golding, B. T.; Radom., L. *J. Am. Chem. Soc.* **2006**, *128*, 3433.

(53) Eagar, R. G., Jr.; Bachovchin, W. W.; Richards, J. H. *Biochemistry* **1975**, *14*, 5523.

(54) Frey, P. A.; Karabatsos, G. L.; Abeles, R. H. *Biochem. Biophys. Res. Commun.* **1965**, *18*, 551.